

State Estimation in Unbalanced Distribution Networks by Symmetrical Components

Amin Dadashzade¹, Shahab Bahrami², and Farrokh Aminifar^{*3}

^{1&3} Electrical and Computer Engineering Department, University of Tehran, Tehran, North Kargar st., P. O. Box: 14395-515, Iran

² Electrical and Computer Engineering Department, University of British Columbia, Vancouver, 5500-2332 Main Mall, P. O. Box: V6T 1Z4, Canada

³ Electrical and Computer Engineering Department, Illinois Institute of Technology, 10 West 35th Street, Chicago, IL, P. O. Box: 60616-3793, USA,

* faminifar@ut.ac.ir

Abstract: State estimation (SE) of a power distribution network plays a vital role in the distribution management systems (DMSs). SE results can monitor and counteract grid technical challenges like tracking the unbalanced operation condition. In this paper, we propose a new approach for unbalanced distribution system SE which is based on the decomposition of the original problem into three subproblems by applying the symmetrical components. The subproblems are of lower dimensions and solved in parallel leading to much less computation time. The convex relaxation method is applied to address nonconvex ac power flow equations and formulate the distribution network SE problem as a semidefinite program (SDP). Furthermore, an algorithm is proposed to detect and attenuate bad data in measurements along with the SE solution. The proposed unbalanced distribution system SE approach is applied to the IEEE 37- and 123-node distribution test systems. The results are compared with those of three-phase SDP-based and linearized SE methods. The superiority of proposed approach is verified in terms of computation time and accuracy.

Keywords: State estimation; unbalanced network; distribution network; situational awareness; bad data detection; PMU measurement; SDP-based optimization.

1. Introduction

THE distribution network in its changing landscape towards the smart grid has manifested challenges associated with the growing penetration of distributed generation, power quality concerns, and system control issues [1, 2]. The situational awareness of the power distribution systems, which utilizes state estimation (SE) analysis, can provide proper information to address these challenges [3]. SE is the process of approximating the power system states based on the network measurements. SE analysis has a crucial role in the distribution management system (DMS) to monitor the operating condition, analyze the security, and control the network [4].

Although SE has been employed in transmission systems for many years, it cannot directly be used in distribution networks due to their special characteristics. First, distribution networks are usually being operated in an unbalanced condition; hence, a single-phase equivalent model is no longer valid and a three-phase SE model must be utilized. Second, lack of sufficient measurements in distribution networks forces DMS to use pseudo and virtual measurements for observability [5, 6], which have extremely different accuracies. In addition, existing measurement devices with very different accuracies cause convergence issues due to matrices ill-conditioning [5]. Third, the high resistance to reactance ratio of power distribution lines makes it impossible to use the decoupled power flow equations in the distribution network SE analyses. Furthermore, in a distribution network, a small amount of power is usually transferred over a short distance and the system states do not vary significantly. The SE analysis accuracy hence poses a great importance. As a result, it is inevitable to use full ac power flow equations. In recent years, the distribution network SE analysis has attracted lots of research interests [7, 8, 9].

Distribution system SE can be divided into two categories of dynamic SE [10, 11] and static SE [12]. In terms of static SE, the earlier research papers on distribution system SE focused on the conventional Newton-Raphson method [13, 14, 15]. The iterative Gauss-Newton solution faces convergence issues and numerical instability due to distribution network aforementioned characteristics. Haughton et al. in [16] presented a linear three-phase distribution system SE to avoid ill-conditioning. Although linear methods have a fast convergence rate, they are weak in terms of accuracy. Recently, new approaches based on the convexification of distribution system SE equations were proposed in literatures. Weng et al. in [17] applied semidefinite programming (SDP) to transmission system SE to convexify the power flow equations. Zhu et al. in [18] devised a distributed SDP-based SE for transmission systems to address computational challenges. Yao et al. in [19] proposed a SDP-based three-phase distribution system SE, which incorporated the three-phase equations in distribution network SE analysis for improving the numerical features. SDP-based distribution network SE suffers from the high computation time while it demonstrates better accuracy. To address the high computation time, references [20, 21] proposed a symmetrical components-based decomposition for distribution system SE problem. Lin et al. in [22] proposed a decentralized method to address the computational efficiency of distribution network SE.

It is worth mentioning that in the distribution network SE literature, several methods have been proposed to utilize branch current for SE analysis [23]. The drawback of the existing branch current-based SE methods is numerical instability issue of the Gauss-Newton solver driven by the ill-conditioned matrix during the solution iteration.

In the light of the literature review, it is evident that having a distribution network SE algorithm with reasonable computational burden and decent accuracy is still wanted. In addition, the robustness of the proposed distribution network SE against the presence of bad data is of great importance. In this paper, we utilize the symmetrical component-based decomposition and SDP-based convexification approach for the distribution system SE problem. The efficiency of SDP to address the numerical instability caused by traditional SE methods and its accuracy has motivated us to use this approach in solving the SE problem in unbalanced distribution networks. The main contributions of this paper are listed as follows:

- *Analysis of the convexified symmetrical components-based SE model:* We examined a new approach for the SE in distribution networks based on decomposing the SE problem into three positive, negative, and zero sequence components by using a convex relaxation technique and transforming the original nonconvex subproblems into an SDP.
- *Computation Time Reduction:* The resultant SE subproblems have lower dimensions in comparison with the original problem; they are hence solved in parallel to lessen the computation complexity while maintaining accuracy.
- *Bad Data Detection and Mitigation:* We propose an algorithm to identify bad data along with the SE process. The proposed algorithm reduces bad data effects on final SE results where it is not required to re-execute the SE after the elimination of bad data.

This paper is organized as follows. Section 2 introduces the system model. In Section 3, the distribution network SE problem is formulated as a SDP. Section 4 proposes the distribution network SE algorithm. Section 5 presents case studies and Section 6 concludes the paper.

2. System Model

Consider an unbalanced three-phase distribution network comprising a set of nodes $\mathcal{N} = \{1, \dots, N\}$ and a set of branches $\mathcal{L} = \{(n, l) | n, l \in \mathcal{N}\}$. In this paper, we utilize μ PMU measurement infrastructure. Let $\mathcal{N}^{\text{PMU}} \subseteq \mathcal{N}$ and $\mathcal{L}^{\text{PMU}} \subseteq \mathcal{L}$ denote the sets of nodes and lines containing μ PMUs measurements that directly calculate node voltage and line current phasors, respectively. These measurements enable us to perform vector decompositions using Fortescue transformation. The limited number of measurements requires pseudo and virtual measurements in DMS for maintaining the distribution network observability. Pseudo measurements are historical DMS data. Let $\mathcal{N}^{\text{psd}} \subseteq \mathcal{N}$ and $\mathcal{L}^{\text{psd}} \subseteq \mathcal{L}$ denote sets of nodes and lines, respectively, which provide pseudo measurements in SE analyses. Also, virtual measurements are exact measurements with zero power injections into nodes and zero power flows in open lines. Let $\mathcal{N}^{\text{vir}} \subseteq \mathcal{N}$ and $\mathcal{L}^{\text{vir}} \subseteq \mathcal{L}$ denote the sets of nodes and lines with virtual measurements in the SE analysis.

We apply the Fortescue transformation to the three-phase voltages and currents to derive the associated symmetrical components. It is worth noting that in four-wire distribution networks, three-phase components are achieved by using Kron reduction method [24]. We then decompose the three-phase distribution network SE problem into three subproblems associated with positive, negative, and zero sequences. It is assumed that the power transmission lines have a symmetrical configuration. In this way, three symmetrical components are decoupled and can be analyzed separately (in Section 5, sensitivity analysis has carried out). Hereafter, we focus on the SE analysis for positive sequence which is denoted by superscript $+$. The SE for the negative and zero sequences can be formulated in a similar fashion. For parts with a single or two phases, virtual two or a single phase is considered, respectively. In other words, for absent phases, we assume virtual phases with zero current on branches and hence the same voltage with upstream node, which enables us to reach three-phase mode to perform Fortescue transformation and symmetrical-component based state estimation decomposition in these networks.

Let $v_n^+ = v_{n,\text{Re}}^+ + jv_{n,\text{Im}}^+$ denote the positive sequence of voltage phasor at node $n \in \mathcal{N}$ and i_{nl}^+ denote the positive sequence of current phasor at line $(n, l) \in \mathcal{L}$. Utilizing the symmetrical components of μ PMU measurements, we determine the positive sequence of power flow through line $(n, l) \in \mathcal{L}$ as $P_{nl}^+ + jQ_{nl}^+ = v_n^+ i_{nl}^{*+}$, where $*$ is the conjugate operation. Also, we determine the positive sequence of the injected power into node $n \in \mathcal{N}$ as $P_{n,\text{inj}}^+ + jQ_{n,\text{inj}}^+ = v_n^+ \sum_{l \in \mathcal{N}} i_{nl}^{*+}$. Let $\mathcal{M} = \{1, \dots, M\}$ denote the set of SE measurements in the sets \mathcal{N}^{PMU} , \mathcal{N}^{psd} , \mathcal{L}^{PMU} , and \mathcal{L}^{psd} . Let $\mathbf{z}^+ = (z_m^+, m \in \mathcal{M})$ denote the vector of positive sequence measurements where z_m^+ is equal to either $v_{n,\text{Re}}^+$, $v_{n,\text{Im}}^+$, P_{nl}^+ , Q_{nl}^+ , $P_{n,\text{inj}}^+$, or $Q_{n,\text{inj}}^+$. The SE analysis will obtain the system state variable vector \mathbf{v}^+ , where $\mathbf{v}^+ = (v_n^+, n \in \mathcal{N})$.

For SE, each measurement z_m^+ is expressed as:

$$z_m^+ = f_m(\mathbf{v}^+) + \varepsilon_m^+, \quad \forall m \in \mathcal{M}, \quad (1)$$

where ε_m^+ is the measurement error $m \in \mathcal{M}$ and function $f_m(\cdot)$ calculates the value measured by measurement m in terms of the system state vector \mathbf{v}^+ . Function $f(\cdot)$ is obtained from the full ac power flow equations and hence is nonlinear and nonconvex for some measurements. To overcome the nonconvexities of the distribution network SE, we formulate SE as a

SDP. Reference [25] can be referenced by interested readers to get an insight into the SDP-based optimization. To derive $f(\cdot)$ and the objective function for SDP, we define the state vector for the positive sequence as follows:

$$\mathbf{x}^+ = [\text{Re}\{\mathbf{v}^+\}^T \text{Im}\{\mathbf{v}^+\}^T]^T. \quad (2)$$

Also, we define variable matrix $\mathbf{W}^+ = \mathbf{x}^+ \mathbf{x}^{+T}$. For $n \in \mathcal{N}$, let e_n denote the n^{th} basis vector in \mathcal{R}^N . To accommodate μ PMU phase angle measurements in SE analyses, we define:

$$\mathbf{R}_n = \begin{bmatrix} e_n e_n^T & \mathbf{0}_{N \times N} \\ \mathbf{0}_{N \times N} & \mathbf{0}_{N \times N} \end{bmatrix}, \quad (3a)$$

$$\mathbf{I}_n = \begin{bmatrix} \mathbf{0}_{N \times N} & \mathbf{0}_{N \times N} \\ \mathbf{0}_{N \times N} & e_n e_n^T \end{bmatrix}. \quad (3b)$$

In Appendix A, we show that:

$$|v_{n,\text{Re}}^+| = \sqrt{\text{Tr}\{\mathbf{R}_n \mathbf{W}^+\}}, \quad \forall n \in \mathcal{N}, \quad (4a)$$

$$|v_{n,\text{Im}}^+| = \sqrt{\text{Tr}\{\mathbf{I}_n \mathbf{W}^+\}}, \quad \forall n \in \mathcal{N}, \quad (4b)$$

where Tr is matrix trace operator. We use the π -equivalent line model for transmission lines [26]. Let Y denotes the system admittance matrix using the line series and shunt impedances, represented by y_{nl} and \bar{y}_{nl} , respectively. We define $Y_n = e_n e_n^T Y$ and $Y_{nl} = (\bar{y}_{nl} + y_{nl}) e_l e_l^T - (y_{nl}) e_n e_n^T$. In addition, for $n \in \mathcal{N}$ and $(n, l) \in \mathcal{L}$, we define matrices \mathbf{Y}_n , $\bar{\mathbf{Y}}_n$, \mathbf{Y}_{nl} , and $\bar{\mathbf{Y}}_{nl}$ as follows:

$$\mathbf{Y}_n = \frac{1}{2} \begin{bmatrix} \text{Re}\{Y_n + Y_n^T\} & \text{Im}\{Y_n^T - Y_n\} \\ \text{Im}\{Y_n - Y_n^T\} & \text{Re}\{Y_n + Y_n^T\} \end{bmatrix}, \quad (5a)$$

$$\bar{\mathbf{Y}}_n = \frac{-1}{2} \begin{bmatrix} \text{Im}\{Y_n + Y_n^T\} & \text{Re}\{Y_n - Y_n^T\} \\ \text{Re}\{Y_n^T - Y_n\} & \text{Im}\{Y_n + Y_n^T\} \end{bmatrix}, \quad (5b)$$

$$\mathbf{Y}_{nl} = \frac{1}{2} \begin{bmatrix} \text{Re}\{Y_{nl} + Y_{nl}^T\} & \text{Im}\{Y_{nl}^T - Y_{nl}\} \\ \text{Im}\{Y_{nl} - Y_{nl}^T\} & \text{Re}\{Y_{nl} + Y_{nl}^T\} \end{bmatrix}, \quad (5c)$$

$$\bar{\mathbf{Y}}_{nl} = \frac{-1}{2} \begin{bmatrix} \text{Im}\{Y_{nl} + Y_{nl}^T\} & \text{Re}\{Y_{nl} - Y_{nl}^T\} \\ \text{Re}\{Y_{nl}^T - Y_{nl}\} & \text{Im}\{Y_{nl} + Y_{nl}^T\} \end{bmatrix}. \quad (5d)$$

Accordingly, we have [17]:

$$P_{n,\text{inj}}^+ = \text{Tr}\{\mathbf{Y}_n \mathbf{W}^+\}, \quad \forall n \in \mathcal{N}, \quad (6a)$$

$$Q_{n,\text{inj}}^+ = \text{Tr}\{\bar{\mathbf{Y}}_n \mathbf{W}^+\}, \quad \forall n \in \mathcal{N}, \quad (6b)$$

$$P_{nl}^+ = \text{Tr}\{\mathbf{Y}_{nl} \mathbf{W}^+\}, \quad \forall (n, l) \in \mathcal{L}, \quad (6c)$$

$$Q_{nl}^+ = \text{Tr}\{\bar{\mathbf{Y}}_{nl} \mathbf{W}^+\}, \quad \forall (n, l) \in \mathcal{L}. \quad (6d)$$

In (4) and (6), it is shown that all measurements can be derived out of variable matrix \mathbf{W}^+ using defined matrices. Let $f_m(\mathbf{W}^+)$ denote the function that relate matrix \mathbf{W}^+ to the measurement $m \in \mathcal{M}$. The vector of measurements \mathbf{z}^+ used in SE comprises μ PMU and pseudo measurements. In contrast, exact virtual measurements appear in SDP as constraints for the SE analyses. These constraints are stated as follows:

$$\text{Tr}\{\mathbf{Y}_n \mathbf{W}^+\} = 0, \quad \forall n \in \mathcal{N}^{\text{vir}}, \quad (7a)$$

$$\text{Tr}\{\bar{\mathbf{Y}}_n \mathbf{W}^+\} = 0, \quad \forall n \in \mathcal{N}^{\text{vir}}, \quad (7b)$$

$$\text{Tr}\{\mathbf{Y}_{nl} \mathbf{W}^+\} = 0, \quad \forall (n, l) \in \mathcal{L}^{\text{vir}}, \quad (7c)$$

$$\text{Tr}\{\bar{\mathbf{Y}}_{nl} \mathbf{W}^+\} = 0, \quad \forall (n, l) \in \mathcal{L}^{\text{vir}}. \quad (7d)$$

Equations (7a) and (7b) correspond to the zero-injection active and reactive powers in node n , respectively. Equations (7c) and (7d) are related to the active and reactive power flows on the open line $(n, l) \in \mathcal{L}$, respectively. In the following section, we discuss the objective function and the constraints of the SDP-based SE analysis.

3. Proposed SE Formulation

We use the weighted least square (WLS) criterion to solve the distribution network SE problem. In this method, the objective is to minimize sum of the squares of differences between estimated variables and available measurements. We define

σ_m as the standard deviation of measurement m . A measurement with a smaller σ_m will have high trustworthy and a larger weight during SE. The objective function for SE is stated as follows:

$$\mathcal{F}^{\text{obj}^+} = \sum_{m \in \mathcal{M}} \frac{1}{\sigma_m^2} \left(z_m^+ - f_m(\mathbf{W}^+) \right)^2. \quad (8)$$

Schur complement theory is used [25] to convert the quadratic objective function (8) to the linear weighted one. We define an auxiliary variable vector $\mathbf{b}^+ \in \mathcal{R}^{M \times 1}$. Accordingly, the distribution network SE problem is formulated as follows:

$$\underset{\mathbf{W}^+, \mathbf{b}^+}{\text{minimize}} \quad \mathcal{F}^{\text{obj}^+} = \sum_{m \in \mathcal{M}} \frac{1}{\sigma_m^2} b_m^+, \quad (9a)$$

$$\text{subject to} \quad \begin{bmatrix} b_m^+ & z_m^+ - f_m(\mathbf{W}^+) \\ z_m^+ - f_m(\mathbf{W}^+) & 1 \end{bmatrix} \succeq 0, \quad (9b)$$

$$(7a) - (7d), \quad (9c)$$

$$\mathbf{W}^+ \succeq 0, \quad (9d)$$

$$\text{rank}(\mathbf{W}^+) = 1. \quad (9e)$$

Constraint (9d) forces matrix \mathbf{W}^+ to be positive semidefinite and (9e) determines that matrix \mathbf{W}^+ is rank-one. Solving problem (9) is challenging since the rank-one constraint (9e) makes problem (9) to be nonconvex. Moreover, in practice, bad data measurements can affect the SE results. Hence, a simultaneous bad data detection and attenuation in SE will be of great value. In the following, we focus on addressing the aforementioned challenges.

3.1. Rank Reduction

The problem expressed by (9) is nonconvex due to the rank-one constraint (9e). We apply the convex relaxation technique to transform (9) into a convex optimization problem. Subsequently, we apply the rank reduction technique to achieve a rank-one solution. In [19], a projection method for rank reduction was deployed, where the rank-one results were obtained using the largest eigenvalue decomposition. Mathematically speaking, in projection method we have:

$$\mathbf{W}^{+\text{opt}} = \lambda_1 \mathbf{K}_1 \mathbf{K}_1^T, \quad (10)$$

where λ_1 is the largest eigenvalue of \mathbf{W}^+ , and \mathbf{K}_1 is the corresponding eigenvector. This method is fast but has a low accuracy drawback. Since the network states in distribution networks do not vary significantly, the accuracy of SE analyses is of great importance and cannot be sacrificed. As a result, a technique which offers more accurate results even with a higher computational burden is preferred. Complying with these features, the convex iteration optimization-based rank reduction approach is proposed in [19] to achieve low-rank solutions. This method finds a matrix $\tilde{\mathbf{W}}$ with a lower rank than the original solution matrix \mathbf{W}^+ . In other words,

$$\text{null}(\mathbf{W}^+) \subseteq \text{null}(\tilde{\mathbf{W}}). \quad (11)$$

The convex iteration method is derived using Theorem 1:

Theorem 1[19]: *If SDP problem is feasible, the solution with the lowest rank must be an extreme point of its feasible set.*

According to Theorem 1, a penalty term is added to the objective function of (9) to reach the extreme point of \mathbf{W}^+ . This term forces the results toward the lowest rank \mathbf{W}^+ by the direction matrix \mathbf{D}^+ , which is the solution of another SDP in (13). Thus, the distribution network SE problem is stated as:

$$\underset{\mathbf{W}^+, \mathbf{b}^+}{\text{minimize}} \quad \sum_{m \in \mathcal{M}} \frac{1}{\sigma_m^2} b_m^+ + \beta^+ \text{Tr}\{\mathbf{W}^{+\text{T}} \mathbf{D}^{+\text{*}}\}, \quad (12a)$$

$$\text{subject to} \quad \begin{bmatrix} b_m^+ & z_m^+ - f_m(\mathbf{W}^+) \\ z_m^+ - f_m(\mathbf{W}^+) & 1 \end{bmatrix} \succeq 0, \quad (12b)$$

$$(7a) - (7d), \quad (12c)$$

$$\mathbf{W}^+ \succeq 0, \quad (12d)$$

where β^+ is a positive weight and $\mathbf{D}^{+\text{*}}$ is the direction matrix derived from the following SDP-based optimization problem:

$$\underset{\mathbf{D}^+}{\text{minimize}} \quad \text{Tr}\{\mathbf{W}^{+\text{*T}} \mathbf{D}^+\}, \quad (13a)$$

subject to

$$0 \preceq \mathbf{D}^+ \preceq \mathbf{I}, \quad (13b)$$

$$\text{Tr}\{\mathbf{D}^+\} = 2N - 1. \quad (13c)$$

In (13a), \mathbf{W}^+ refers to the solution of (12). Constraints (13b) - (13c) force the direction matrix to be in the convex hull of all rank $2N - 1$ orthogonal matrices and by optimization, we look for extreme points of the set. This iteration will continue until the rank-one condition is achieved. In calculations, we consider it as:

$$\text{Tr}\{\mathbf{W}^{+T} \mathbf{D}^{+*}\} = 0. \quad (14)$$

Equation (14) implies that the $2N - 1$ eigenvalues of matrix \mathbf{W}^+ should be zero to obtain the rank-one solution. The rank-one solution derives the positive sequence voltage components using \mathbf{W}^+ . We use the following equations to extract the system states.

$$v_n^+ = \sqrt{\text{Tr}\{\mathbf{R}_n \mathbf{W}^+\} + \text{Tr}\{\mathbf{I}_n \mathbf{W}^+\}}, \quad (15a)$$

$$\theta_n^+ = \tan^{-1} \left(\frac{\sqrt{\text{Tr}\{\mathbf{I}_n \mathbf{W}^+\}}}{\sqrt{\text{Tr}\{\mathbf{R}_n \mathbf{W}^+\}}} \right). \quad (15b)$$

The proof is given in Appendix B.

For negative and zero sequences SE, voltage phase angles are sometimes greater than 90 degrees which correspond to the negative real part of the solution. To detect this condition, we use the non-diagonal components of \mathbf{W}^- and \mathbf{W}^0 , respectively. These components consist of the products of real and imaginary voltages. If this value for a given node of the system is negative, its angle is greater than 90 degrees. In order to calculate the system states using the proposed optimization problem, we first use (15a) and (15b) to calculate the system positive, negative, and zero states separately from \mathbf{W}^+ , \mathbf{W}^- , and \mathbf{W}^0 . Then, we apply the inverse Fortescue transform to the symmetrical component SE to determine the three-phase system states. Using the symmetrical components, we reduce dimension of \mathbf{W}^+ from $6N \times 6N$ to $2N \times 2N$; hence, the calculation of rank-one results by the direction matrix \mathbf{D}^+ leads to a lower approximation error [27].

In the zero sequence SE, some sorts of distribution network transformer connection, say wye, force zero sequence components to be zero. These values are incorporated in the models as virtual measurements.

3.2. Bad Data Detection

In this section, we show that the system states in nodes with μ PMUs can be extracted before the iterative rank reduction process. To do so, we build the principal submatrix $\mathbf{W}_{(s)}^+$, where set \mathcal{S} relates to the row numbers in the matrix \mathbf{W}^+ that are associated with measurement nodes. The principal submatrix is made by retaining the liked-numbered rows and columns in set \mathcal{S} . By building the principal submatrix, we divide \mathbf{W}^+ into $\mathbf{W}_{(s)}^+$ and $\mathbf{w}_{(k)}^+$ where set \mathcal{K} is associated with row numbers in the matrix \mathbf{W}^+ that do not have measurement devices. According to proposition on the rank decomposition [28], $\text{rank}(\mathbf{W}^+) = \text{rank}(\mathbf{W}_{(s)}^+) + \text{rank}(\mathbf{w}_{(k)}^+)$. In the following, we focus on the principal submatrix $\mathbf{W}_{(s)}^+$ rank.

Sufficient conditions in which a rank-one result can be achieved are [19]: i) the network operates in balanced mode; ii) measurements are without noise; iii) all nodes have voltage measurements. Among the aforementioned conditions for the principal submatrix, the first condition is met in our formulation since we utilize a Fortescue transform to convert an unbalanced network into three balanced positive, negative, and zero sequence networks [29]. For the second, we used a method proposed in [30, 31] to extract the rank-one matrix out of noisy measurements. For the third, according to reference [19], one of the sufficient conditions for obtaining rank-one result is the availability of voltage magnitude measurements in all nodes. We know that it is not the case in real distribution networks to have measurement at all nodes of the distribution network. So, some rows and columns of the matrix \mathbf{W}^+ do not contain measurements. To solve this problem, we create matrix $\mathbf{W}^+(s)$ which contains just the rows and columns of the matrix \mathbf{W}^+ that contain the measurement facilities. In this condition, we met one of the sufficient conditions to achieve the rank one output results. Mathematically speaking, the principal submatrix contains only the nodes that have measurement equipment. The principal submatrix $\mathbf{W}_{(s)}^+$ covers all the above three conditions and has a rank-one characteristics which enables us to extract power system states in nodes with μ PMU measurements before the rank reduction process [32].

Using the states obtained from (15) and its corresponding negative and zero sequence states, we perform the inverse Fortescue transform to calculate the residual for a given measurement $m \in \mathcal{M}$. The residual is the differences between measurements and their estimated values, and its normalized value is calculated as follows:

$$R_m = \left| \frac{z_m - z_m^{est}}{\sigma_m} \right|, \quad (16)$$

where z_m^{est} is the estimated value associated with the measured value z_m of the distribution network.

The imprecise network model and inexact measurements cause nonzero residuals in SE analyses. The presence of bad data, which could be due to intrusions or faults within measurement infrastructures, increases the related residual, which can seriously affect the SE results. We assume the errors have a Gaussian probability density function (PDF) with zero mean.

Along with the calculation of SE and before rank reduction process, we construct $\mathbf{W}_{(s)}^+$ and calculate the residuals. If the measurement residual $m \in \mathcal{M}$ is higher than the threshold $(\pm 3\sigma_m)$, it is known as bad data with a confidence level of 99% [4]. By extracting the measurement residuals before rank reduction process, we determine bad data in measurements and reduce their weights in SE.

The innovation of the proposed method in comparison to the available bad data detection methods is that it can detect and attenuates the bad data simultaneously with SE analysis. In available methods, if any bad data is detected, it should be removed from the input data and SE needs to be re-executed and this process might be iterated several times until no suspected bad data is flagged. In this paper, using the characteristics of the rank reduction algorithm, we calculate the normalized residuals of the network measurement along with solving SE problem, and we can detect the presence of bad data simultaneously. Thereafter, the weights of suspected measurements are adjusted to diminish their effects.

4. Proposed Algorithm Design

Algorithm 1 depicts the proposed three-phase unbalanced distribution network SE for the positive sequence. The algorithm for the other negative and zero sequences are the same. In Line 1, we form the SE analysis positive sequence measurement vector \mathbf{z}^+ which consist of pseudo and μ PMU measurements. In Line 2, using the SDP SE formulation, we relax the nonconvex rank-one constraint (9e) and solve (9) for the positive sequence component. We next form $\mathbf{W}_{(s)}^+$ to derive normalized residuals in Line 4 using (16). Using the residuals from Line 4, we search for bad data based on the threshold discussed in Section III and assign new standard deviations to suspicious measurements in Line 5. The weights of related measurements alleviate the adverse effects of bad data on final results. In Line 6, we perform the rank reduction process. We solve (13) to calculate the direction matrix \mathbf{D}^+ so long as the penalty term in the objective function is not zero, and solve (12) to reach lower rank result. In Line 9, we use (15) to calculate positive sequence states. Finally, using the three positive, negative, and zero sequence SE results, we apply the inverse symmetrical component to calculate the distribution network three-phase states.

Algorithm 1 Proposed SE Algorithm.

- 1: Form SE analysis positive sequence measurement \mathbf{z}^+
 - 2: Relax the rank-one constraint (9e) and solve (9) for positive sequence data.
 - 3: Compute the inverse symmetrical components.
 - 4: Form matrix $\mathbf{W}_{(s)}^+$ and compute the measurement residuals in order to detect bad data using (16).
 - 5: Assign new σ_m accuracy weights and set β^+ .
 - 6: **Repeat**
 - 7: Solve problem (12) and update \mathbf{D}^+ by Solving (13).
 - 8: **While** $\text{Tr}\{\mathbf{W}^{+T} \mathbf{D}^{+*}\} = 0$
 - 9: Compute positive sequence states using (15a) and (15b) and calculate inverse Fortescue transform on positive, negative, and zero sequence SE results.
-

5. Numerical Studies

In this section, we demonstrate performance of the proposed method on the IEEE 37- and 123-node test distribution networks. The test systems data can be found in [33]. The only measurement data that we use in the distribution system SE formulation are μ PMUs measurements. The accuracy of the measured values is extracted from the datasheet of a Micro-PMU product, and the associated uncertainties are calculated via the technique presented in [34]. Virtual measurements are supposed to be absolutely exact and managed in the SDP formulation as constraints. In contrast, pseudo measurements are driven from historical data and is used to enhance observability of the SE analysis. These measurements are assumed to have 50% error in the numerical studies. In the simulations, ten percent of nodes are supposed to have pseudo-measurements.

The allocation of μ PMU locations in distribution networks is highly discussed in the literature [35-38]. It should be considered that that the locations of Micro-PMUs in the distribution network are mainly determined based on satisfying the minimum accuracy required to estimate the voltage profile and the visibility of the network is provided using pseudo-measurements. However, a dependable SE bad data detection function needs an extensive set of input data (more than observability requirement) to be overdetermined and to be able to support bad data detection capability. This data is a combination of real measurements, pseudo measurements, and virtual measurements but the more pseudo measurements we have, the less possibility for bad data detection is realized. In the proposed methodology, the simultaneous bad data detection (as opposed to cumbersome convectional approach to run bad data detection/rejection sequentially after the first iteration of SE) is focused as one of the contributions. As a result, we used the placement scheme proposed in reference [39].

The OpenDSS software [40] is used to perform the power flow and generate system measurements. μ PMU precision is 0.05% [41]. We add a normal distribution probability with a zero mean and a variance which is twice the μ PMU precision to accommodate transducer errors. The zero injection nodes are virtual measurements in SE analyses and their locations are shown in Fig. 1. The proposed distribution network SE problem is solved using MATLAB/CVX [42] with Mosek 7 [43] solver in a PC with Intel(R) Core(TM) i7-4710HQ CPU @ 2.5 GHz.

5.1. Accuracy Analysis

In order to evaluate the accuracy of the proposed distribution network SE method, we compare the resulting SE errors with three-phase SDP-based and linear distribution network SE solutions. Percentage form index-based errors are defined as:

$$\text{Amplitude error} = \frac{|v^{\text{estimated}} - v^{\text{true state}}|}{|v^{\text{true state}}|}, \quad (17a)$$

$$\text{Angle error} = \frac{|\theta^{\text{estimated}} - \theta^{\text{true state}}|}{|\theta^{\text{true state}}|}. \quad (17b)$$

Figs. 2(a) and 2(b) depict the SE amplitude and angle errors for the proposed, three-phase SDP-based, and linear methods. Also, the maximum magnitude and angle errors of node voltages are given in Tables 1 and 2. It is deduced that the proposed method is superior in terms of accuracy which is due to the fact that the full ac power flow model is applied. Furthermore, the decomposition of the distribution network SE problem by symmetrical components provides the opportunity of utilizing single-line equivalent models of distribution network. Hence, the dimension of \mathbf{W}^+ is lower than that of the three-phase model and the rank reduction leads to a higher accuracy (Section 3. A). Referring to Table 1, the linear method is the least accurate one due to the approximations in the power flow model. In distribution system SE analysis, accuracy is our first priority. The reason is that in the distribution network, a small amount of power is usually transferred over a short distance and system states do not hence vary significantly, and the SE analyses accuracy poses vital importance. In this paper, we convexified the nonconvex distribution system SE problem to reduce the computation time while maintaining the accuracy. Different SE methods have various characteristics in terms of computation times and accuracy. DSO should decide based on associated preferences.

5.2. Computational Effort

Table 3 compares the SE analysis computation times using the three methods for the 37- and 123-node test systems. Our proposed method reduces the SE process time significantly. For instance, the distribution network SE on the 37-node network takes 63 seconds while for three-phase SDP based-SE takes 27 minutes. Similarly, for 123-node network, the proposed method decreases the computation time by over 100 minutes. This reduction is due to the decomposition of the distribution network SE problem into symmetrical components which reduce the problem dimension and allow parallel processing. Moreover, since we consider the single line network model in symmetrical components, the \mathbf{W}^+ rank will not increase due to unbalanced operating conditions. Hence, rank reduction is done faster. In Table 3, the computation time of the proposed method is more than the linear method because the proposed method applies the full ac power flow. This cost is however justified by the higher accuracy gained.

5.3. Bad Data Detection

It should be noted that for the detection of bad data, the redundancy of measured data must be granted. According to Fig. 1, we add two μ PMUs at nodes 3 and 13. In order to evaluate the proposed bad data detection approach, we use the 37-node network and add 0.2 (p.u.) to voltage measurements at node 2, active power measurement at node 13, and reactive power measurement at node 23. Utilizing the normalized measurement residuals with a 99% confidence level, the bad data threshold is set to 3. The bad data are represented by absolute measurement residuals that exceed the threshold. The measurements in the 37-node network are numbered as outlined in Table 4. Figs. 3 and 4 depict the normalized residuals of voltages and active and reactive powers in the absence of bad data, presence of bad data, and with the bad data removal, respectively. Also, Tables 5 to 7 show the maximum and the aggregation of normalized residuals of voltage, active power, and reactive power measurements, respectively. As shown in Figs. 3(a) and 4(a), the normalized measurement residuals without bad data is less than the prescribed threshold. After the bad data injection on nodes 2, 13, and 23, the residuals exceed the threshold. The maximum normalized residuals for voltage, active power, and reactive power are 18.1, 10.91, and 10.9, respectively, which shows significant increase of SE residuals. They are hence treated as bad data in the following rank reduction process.

According to Figs. 3(b) and 4(b), bad data measurements increase voltage measurement residuals and boost residual in nearby nodes. To attenuate the bad data effect on the distribution network SE results, we divide the measurement weights by 100 and then start the rank reduction process. Figs. 3(c) and 4(c) illustrate the normalized residuals after the bad data attenuation process for voltage, active power, and reactive power. According to Table 5, the maximum and the sum of voltage measurement residuals after bad data attenuation are reduced by 15.8 and 32.22, respectively. Also, according to Tables 6 and

7, the maximum normalized active and reactive powers are decreased by 9.63 and 9.5, respectively, which shows that the proposed method can efficiently detect and attenuate the bad data in SE analysis.

In other scenario, we use the 37-bus network and add 0.4 (p.u.) to voltage measurements at bus 2, active power measurement at bus 13, and reactive power measurement at bus 23. According to Table 8, the maximum and the sum of voltage measurement residuals after bad data attenuation are reduced by 32.15 and 108.35, respectively. Also, according to Tables 9 and 10, the maximum normalized active and reactive powers are decreased by 19.75 and 18.37, respectively.

5.4. Untransposed Lines

In developing the proposed method, we supposed distribution network lines have symmetrical configurations (i.e., impedance matrices of symmetrical components are diagonal). However, in practice this condition may not hold. Hence, the symmetrical components of the distribution network are coupled [44]. Mathematically speaking, the voltage drop equation for a branch in general form is as follows [45]:

$$\begin{bmatrix} \Delta V_a \\ \Delta V_b \\ \Delta V_c \end{bmatrix} = \begin{bmatrix} Z_{11} & Z_{12} & Z_{13} \\ Z_{21} & Z_{22} & Z_{23} \\ Z_{31} & Z_{32} & Z_{33} \end{bmatrix} \times \begin{bmatrix} I_a \\ I_b \\ I_c \end{bmatrix} \quad (18)$$

Converting above equation into symmetrical components [45], we have:

$$Z_{012} = \begin{bmatrix} (Z_{s0} + 2Z_{M0}) & (Z_{s2} - Z_{M2}) & (Z_{s1} - Z_{M1}) \\ (Z_{s1} - Z_{M1}) & (Z_{s0} - Z_{M0}) & (Z_{s2} + 2Z_{M2}) \\ (Z_{s2} - Z_{M2}) & (Z_{s1} + 2Z_{M1}) & (Z_{s0} - Z_{M0}) \end{bmatrix} \quad (19)$$

Where:

$$Z_{s0} = \frac{1}{3}(Z_{11} + Z_{22} + Z_{33}) \quad (20)$$

$$Z_{s1} = \frac{1}{3}(Z_{11} + aZ_{22} + a^2Z_{33})$$

$$Z_{s2} = \frac{1}{3}(Z_{11} + a^2Z_{22} + aZ_{33})$$

$$Z_{M0} = \frac{1}{3}(Z_{12} + Z_{23} + Z_{13}) \quad (21)$$

$$Z_{M1} = \frac{1}{3}(Z_{12} + aZ_{23} + a^2Z_{13})$$

$$Z_{M2} = \frac{1}{3}(Z_{12} + a^2Z_{23} + aZ_{13})$$

When the branch is transposed, the symmetrical components-based impedance can be demonstrated as follows:

$$Z_{M0} = A, Z_{M1} = Z_{M2} = 0, \quad (22)$$

$$Z_{s0} = B, Z_{s1} = Z_{s2} = 0,$$

$$Z_{012} = \begin{bmatrix} (B + 2A) & 0 & 0 \\ 0 & (B - A) & 0 \\ 0 & 0 & (B - A) \end{bmatrix}$$

In an ideally transposed configuration, different sequence components are decoupled, and the symmetrical component current of each type (positive, negative, and zero) will cause the voltage drop of the same kind [46]. In our proposed method, by assuming the lines as transposed ones, we have neglected the off-diagonal elements of the impedance matrix. To analyse the error of this assumption, first, we perform the SE analysis on a distribution network that has untransposed line configurations. In the second step, we change the line parameters into a transposed line configuration and execute the SE analysis. In the third step, we calculate the associated SE errors of desired case with transposed branches against the real case having untransposed lines. This way, we will have insight into the errors introduced by the assumption of transposed branch configurations.

Figs. 5(a) and 5(b) depict the magnitude and angle errors of node voltages, respectively. In Fig. 5, the proposed method offers a negligible error in the magnitude and angle of untransposed node voltages in comparison with the transposed mode. This is because the off-diagonal elements of the impedance matrices of symmetrical components are negligibly small in comparison with the diagonal terms.

6. Conclusion

In this paper, we examined the performance of the symmetrical component-based approach for SE analysis in unbalanced distribution networks. A convexified approach based on the SDP method was developed to tackle the distribution network SE problems associated with the positive, negative, and zero sequence circuits. The relaxation technique was taken in use to accommodate the only nonconvex rank one constraint. Finally, a novel approach was proposed for bad data detection and attenuation. The simulation results on both IEEE 37- and 123-node distribution networks and the comparison with those of three-phase SDP-based SE showed that the SE computation time in the proposed method is drastically lower. In terms of accuracy, the proposed method is superior to the three-phase SDP method. Also, according to the simulation results, it was shown that the proposed method can wisely detect the existence of bad data and attenuate its effects along with solving the distribution network SE problem. This feature relaxes the need for time-consuming multiple SE executions as prescribed in the conventional SE packages.

7. References

- [1] Madani, V. *et al.*, "Distribution automation strategies challenges and opportunities in a changing landscape," *IEEE Trans. on Smart Grid*, 6, (4), pp. 2157-2165 (2015).
- [2] Das, R. *et al.*, "Distribution automation strategies: Evolution of technologies and the business case," *IEEE Trans. on Smart Grid*, 6, (4), pp. 2166-2175 (2015).
- [3] Panteli, M. and Kirschen, D. "Situation awareness in power systems: Theory, challenges and applications," *Electric Power Syst. Research*, 122, pp. 140-151 (2015).
- [4] Primadianto, A. and Lu, C. "A review on distribution system state estimation," *IEEE Trans. on Power Syst.*, 32, (5), pp. 3875-3883 (2016).
- [5] Clements, K. "The impact of pseudo-measurements on state estimator accuracy," in 2011 *IEEE Power and Energy Soc. Gen. Meet.*, 2011, pp. 1-4: IEEE (2011).
- [6] Teimourzadeh, S. Aminifar, F. and Shahidehpour, M. "Contingency-constrained optimal placement of micro-PMUs and smart meters in microgrids," *IEEE Trans. on Smart Grid*, 10, (2), pp. 1889-1897 (2017).
- [7] Wang, G. Giannakis, G. Chen, J. Sun, J. "Distribution system state estimation: An overview of recent developments." *Frontiers of Information Technology & Electronic Engineering*. 20, (1), pp. 4-17. (2019)
- [8] Fotuhi-Friuzabad, M. Safdarian, A. Moeini-Aghaie, *et al.*, "Upcoming challenges of future electric power systems: sustainability and resiliency". *Scientia Iranica*. 23(4), pp. 1565-77 (2016)
- [9] Osbouei, A. Karegar, K. "Power System Thévenin Equivalent Estimation Based on Phasor Measurements". *Scientia Iranica*, 25, (6), pp. 3559-68 (2018)
- [10] Junbo, Z. Netto, M. *et al.*, "Roles of dynamic state estimation in power system modeling, monitoring and operation." *IEEE Trans. on Power Syst.*, 36, (3), pp. 2462-2472 (2020)
- [11] Carlo, M. Pegoraro, P. A. Sullis, S. Pau, *et al.* "New Kalman filter approach exploiting frequency knowledge for accurate PMU-based power system state estimation." *IEEE Transactions on Instrumentation and Measurement* 69, (9), pp. 6713-6722 (2020)
- [12] Ajoudani, M. Shiekholeslami, A. Zakariazadeh, A. "Improving state estimation accuracy in active distribution networks by coordinating real-time and pseudo-measurements considering load uncertainty." *IET Generation, Transmission & Distribution*. 2022. (Early access)
- [13] Lu, C. Teng, J. and Liu, W. "Distribution system state estimation," *IEEE Trans. on Power syst.*, 10, (1), pp. 229-240 (1995).
- [14] Lin, W. and Teng, J. "Distribution fast decoupled state estimation by measurement pairing," *IEEE Proc. Gen., Trans. and Dist.*, 143, (1), pp. 43-48 (1996).
- [15] Lin, W. and Teng, J. "State estimation for distribution systems with zero-injection constraints," in *Proc. of Power Ind. Computer App. Conf.*, pp. 523-529 (1995).
- [16] Houghton, D. and Heydt, G. "A linear state estimation formulation for smart distribution systems," *IEEE Trans. on Power Syst.*, 28, (2), pp. 1187-1195 (2012).
- [17] Weng, Y. Fardanesh, B. Ilic, *et al.* "Novel approaches using semidefinite programming method for power systems state estimation," in *2013 North Am. Power Symp. (NAPS)*, pp. 1-6: IEEE (2013).
- [18] Zhu, H. and Giannakis, G. "Power system nonlinear state estimation using distributed semidefinite programming," *IEEE Journal of Selected Topics in Signal Processing*, 8, (6), pp. 1039-1050 (2014).
- [19] Yao, Y. Liu, X. Zhao, D. and Li, Z. "Distribution system state estimation: A semidefinite programming approach," *IEEE Trans. on Smart Grid*, 10, (4), pp. 4369-4378 (2018).
- [20] Fernandes, T. R. Venkatesh, B. and Almeida, M. C. "Symmetrical Components Based State Estimator for Power Distribution Systems," in *IEEE Transactions on Power Systems*, 36, (3), pp. 2035-2045, (2021)
- [21] Murat, G. "Three-Phase State Estimation Based on Symmetrical Components." In 2020 IEEE PES Innovative Smart Grid Technologies Europe (ISGT-Europe), pp. 186-190. IEEE, (2020)
- [22] Lin, C. Wu, W. and Guo, Y. "Decentralized Ronodet State Estimation of Active Distribution Grids Incorporating Microgrids Based on PMU Measurements," *IEEE Trans. on Smart Grid*, 11, (1), pp. 810-820 (2019).
- [23] Baran, M. Kelley, A. "A branch-current-based state estimation method for distribution systems," in *IEEE Transactions on Power Systems*, 10, (1), pp. 483-91. (1995)
- [24] Kron, G. "Tensorial analysis of integrated transmission systems part I. the six basic reference frames," *Trans. of the Am. Inst. of Electrical Engineers*, 70, (2), pp. 1239-1248 (1951).
- [25] Lavaei, J. and Low, S. H. "Zero duality gap in optimal power flow problem," *IEEE Trans. on Power Syst.*, 27, (1), pp. 92-107 (2011).
- [26] Glover, J. Sarma, M. and Overbye, T. *Power system analysis & design*, SI version. Cengage Learning, 2012.
- [27] Aspremont, A. Ghaoui, L. Jordan, E. *et al.* "A direct formulation for sparse PCA using semidefinite programming," in *Advances in neural information processing systems*, pp. 41-48 (2005).
- [28] Thompson, R. "Principal submatrices V: Some results concerning principal submatrices matrices," *J. Res. Nat. Bur. Standards Sect. B*, 72, (2), pp. 115-125, (1968)

- [29] Fortescue, C. "Method of symmetrical co-ordinates applied to the solution of polyphase networks," *Trans. of the Am. Ins. of Elec. Eng.*, 37, (2), pp. 1027-1140 (1918).
- [30] Boyd, S. Vandenberghe, L. Convex optimization. Cambridge university press, (2004).
- [31] So, A. Ye, Y. and Zhang, J. "A unified theorem on SDP rank reduction," *Math. of Operations Research*, 33, (4), pp. 910-920 (2008).
- [32] Shabalin, A. and Nobel, A. "Reconstruction of a low-rank matrix in the presence of Gaussian noise," *Journal of Multivariate Analysis*, 118, pp. 67-76 (2013)
- [33] (2019-09-30). Available: <http://sites.ieee.org/pestestfeeders/>
- [34] Stewart, E.M. and von Meier, A., 2016. Phasor Measurements for Distribution System Applications.
- [35] Gholami, M. Abbaspour, A. Fattaheian-Dehkordi, *et al.* "Optimal allocation of PMUs in active distribution network considering reliability of state estimation results". *IET Generation, Transmission & Distribution*. 14(18), pp. 3641-51(2020)
- [36] Almeida, D. Fernandes, T. Ugarte. L. State Estimation and Active Distribution Networks. In *Planning and Operation of Active Distribution Networks*, pp. 377-402. Springer, Cham, (2022)
- [37] Farkhondeh, J. Bahmanyar, A. and Shabanzadeh, M. "Optimal Meter Placement in Distribution Feeders Using Branch-Current based Three-Phase State Estimation: A Quest for Observability Enhancement." In *2020 10th Smart Grid Conference (SGC)*, pp. 1-6. IEEE, (2020)
- [38] Aminifar, F. Safdarian, A. Fotuhi-Firuzabad, A. M. Shahidehpour, M. "A multi-objective framework for enhancing the reliability and minimizing the cost of PMU deployment in power systems." *Scientia Iranica*. 2016 Dec 1;23(6):2917-27.
- [39] Kerns, B. "Optimal micro phasor measurement unit placement for complete observability of the distribution system.", University of British Columbia (2018).
- [40] Dugan, R. "Opendss manual," EPRI,[Online] Available at: <http://sourceforge.net/apps/mediawiki/electricdss/index.php>.
- [41] Stewart, E. and von Meier, A. "Phasor measurements for distribution system applications," *Smart Grid Handbook*, pp. 1-10 (2016).
- [42] Grant, M. Boyd, S. and Ye, Y. "CVX: Matlab software for disciplined convex programming," (2009).
- [43] Mosek, A. "The MOSEK optimization software," Online at <http://www.mosek.com>, 54, (2-1), pp. 5-10, (2010).
- [44] Vieira, J. Freitas, W. and Morelato, A. "Phase-decoupled method for three-phase power-flow analysis of unbalanced distribution systems," *IEEE Proc. Gen., Trans. and Dist.*, 151, (5), pp. 568-574 (2004).
- [45] Gonen, T. Electric power distribution engineering. CRC press; 2015 Aug 18.
- [46] Dadashzade, A. Aminifar, F. and Davarpanah, M. "Unbalanced Source Detection in Power Distribution Networks by Negative Sequence Apparent Powers," in *IEEE Transactions on Power Delivery*, 36, 1, pp. 481-483, Feb. (2021)

8. Appendices

8.1. Proof of Equation (4)

In this subsection, we show that how real and imaginary parts of node voltages calculated using the matrix \mathbf{W}^+ . we have defined matrix \mathbf{W}^+ as:

$$\mathbf{W}^+ = \mathbf{x}^+ \mathbf{x}^{+T} = \begin{bmatrix} \text{Re}\{\mathbf{v}^+\} \text{Re}\{\mathbf{v}^+\} & \text{Re}\{\mathbf{v}^+\} \text{Im}\{\mathbf{v}^+\} \\ \text{Im}\{\mathbf{v}^+\} \text{Re}\{\mathbf{v}^+\} & \text{Im}\{\mathbf{v}^+\} \text{Im}\{\mathbf{v}^+\} \end{bmatrix}, \quad (23a)$$

$$= \text{Tr} \left\{ \begin{bmatrix} e_n e_n^T & \mathbf{0}_{N \times N} \\ \mathbf{0}_{N \times N} & \mathbf{0}_{N \times N} \end{bmatrix} \times \begin{bmatrix} \text{Re}\{\mathbf{v}^+\} \text{Re}\{\mathbf{v}^+\} & \text{Re}\{\mathbf{v}^+\} \text{Im}\{\mathbf{v}^+\} \\ \text{Im}\{\mathbf{v}^+\} \text{Re}\{\mathbf{v}^+\} & \text{Im}\{\mathbf{v}^+\} \text{Im}\{\mathbf{v}^+\} \end{bmatrix} \right\}, \quad (23b)$$

$$= \text{Tr} \left\{ \begin{bmatrix} e_n e_n^T \times \text{Re}\{\mathbf{v}^+\} \text{Re}\{\mathbf{v}^+\} & \mathbf{0}_{N \times N} \\ \mathbf{0}_{N \times N} & \mathbf{0}_{N \times N} \end{bmatrix} \right\} \quad (23c)$$

$$|v_{n,\text{Re}}^+| = \sqrt{\text{Tr}\{\mathbf{R}_n \mathbf{W}^+\}} \quad (23d)$$

For the imaginary part, we have:

$$|v_{n,\text{Re}}^+|^2 = \text{Tr} \left\{ \begin{bmatrix} e_n e_n^T \times \text{Re}\{\mathbf{v}^+\} \text{Re}\{\mathbf{v}^+\} & \mathbf{0}_{N \times N} \\ \mathbf{0}_{N \times N} & \mathbf{0}_{N \times N} \end{bmatrix} \right\} \quad (24a)$$

$$|v_{n,\text{Re}}^+| = \sqrt{\text{Tr}\{\mathbf{R}_n \mathbf{W}^+\}} \quad (24b)$$

8.2. Proof of Equation (15)

Based on Appendix 8.1, having both real and imaginary parts of the voltage phasors at node $n \in \mathcal{N}$, we derive system states as follows:

$$v_n^+ = \sqrt{|v_{n,\text{Re}}^+|^2 + |v_{n,\text{Im}}^+|^2} = \sqrt{\text{Tr}\{\mathbf{R}_n \mathbf{W}^+\} + \text{Tr}\{\mathbf{I}_n \mathbf{W}^+\}}, \quad (25a)$$

$$\theta_n^+ = \tan^{-1} \left(\frac{\sqrt{|v_{n,\text{Im}}^+|^2}}{\sqrt{|v_{n,\text{Re}}^+|^2}} \right) = \tan^{-1} \left(\frac{\sqrt{\text{Tr}\{\mathbf{I}_n \mathbf{W}^+\}}}{\sqrt{\text{Tr}\{\mathbf{R}_n \mathbf{W}^+\}}} \right). \quad (25b)$$

Biographies:

Amin Dadashzade received the BSc degree from Urmia University, Urmia, Iran, in 2017, and the MSc from Tehran University, Tehran, Iran, in 2020. He is currently a Ph.D. student at the University of Toronto. His research interests include power system operation analysis and renewable generation integration analysis.

Shahab Bahrami Shahab Bahrami (M'17) received the B.A.Sc. and M.A.Sc. degrees both in Electrical Engineering from Sharif University of Technology, Tehran, Iran, in 2010 and 2012, respectively. He received the Ph.D. degree in Electrical & Computer Engineering from the University of British Columbia (UBC), Vancouver, BC, Canada in 2017. Dr. Bahrami has received various prestigious scholarships at UBC, including the distinguished and highly competitive UBC's Four Year Fellowship (2013–2017) and the Graduate Support Initiative Award from the Faculty of Applied Science at UBC (2014–2017). Currently, he works as a postdoctoral research fellow at UBC. His research interests include convex optimization, machine learning, and deep reinforcement learning with applications to 5G wireless communication and smart grid.

Farrokh Aminifar (Senior Member, IEEE) is currently an Associate Professor with the School of Electrical and Computer Engineering, College of Engineering, University of Tehran, Tehran, Iran, and a Senior Research Associate with the Robert W. Galvin Center for Electricity Innovation, Illinois Institute of Technology, Chicago, IL, USA. He is the recipient of the 2011 IEEE Iran Section Best PhD Dissertation Award, the 2013 IEEE/PSO Transactions Prize Paper Award, the 2015 IEEE Iran Section Young Investigator Award, 2017 Outstanding Young Scientist Award of Iran National Academy of Science, and COMSTECH 2017 Best Young Researcher Award. Dr. Aminifar is an Editor for the IEEE TRANSACTIONS ON POWER SYSTEMS, IEEE POWER ENGINEERING LETTERS, and IET Smart Grid. His current research interests include synchrophasor applications, resilience analysis, and power system optimization.

Figures:

Fig. 1. The 37-node distribution system.

Fig. 2. Estimation error for the IEEE 37-node system: (a) amplitude, (b) angle.

Fig. 3. Residuals of node voltages for the IEEE 37-node system: (a) absence of bad data; (b) presence of bad data; (c) with the bad data removal approach.

Fig. 4. Residuals of active power (triangle markers) and reactive power (diamond markers) for the IEEE 37-node system: (a) absence of bad data; (b) presence of bad data; (c) with bad data removal approach.

Fig. 5. Estimation errors for the IEEE 37-node system: (a) amplitude; (b) angle.

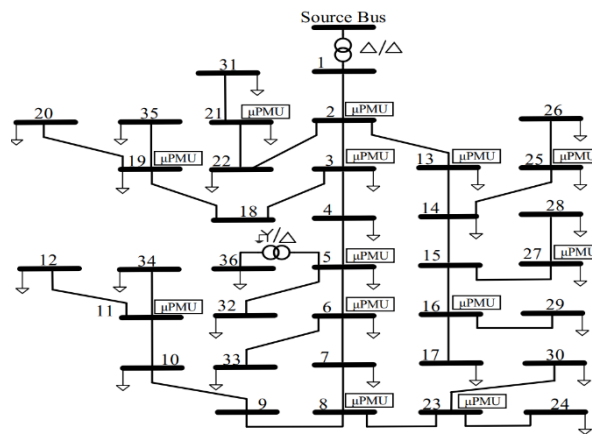
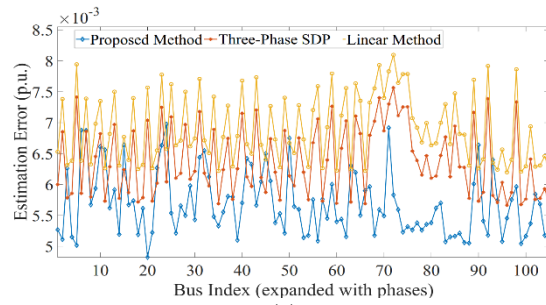
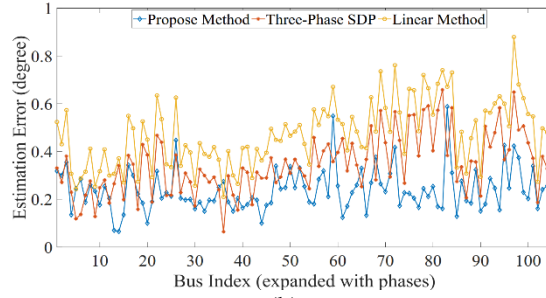


Fig. 1. The 37-node distribution system.

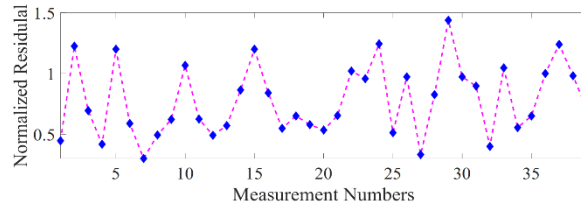


(a)

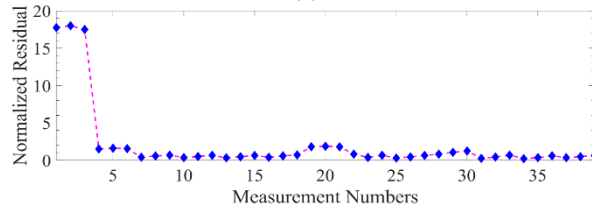


(b)

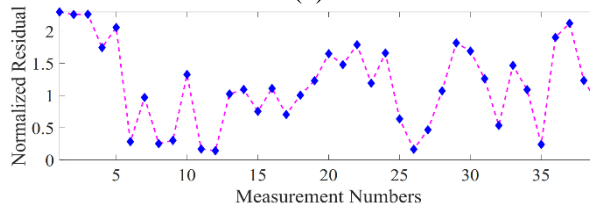
Fig. 2. Estimation error for the IEEE 37-node system: (a) amplitude, (b) angle.



(a)



(b)



(c)

Fig. 3. Residuals of node voltages for the IEEE 37-node system: (a) absence of bad data; (b) presence of bad data; (c) with the bad data removal approach.

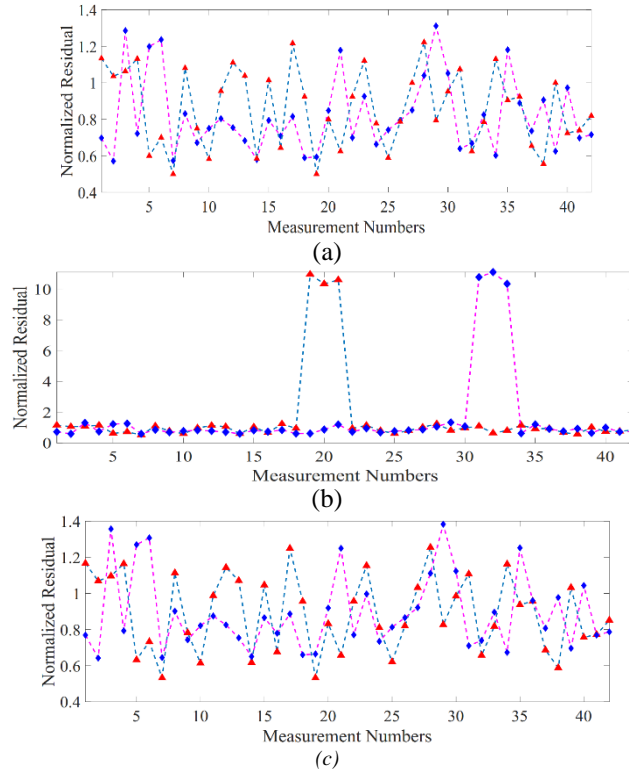


Fig. 4. Residuals of active power (triangle markers) and reactive power (diamond markers) for the IEEE 37-node system: (a) absence of bad data; (b) presence of bad data; (c) with bad data removal approach.

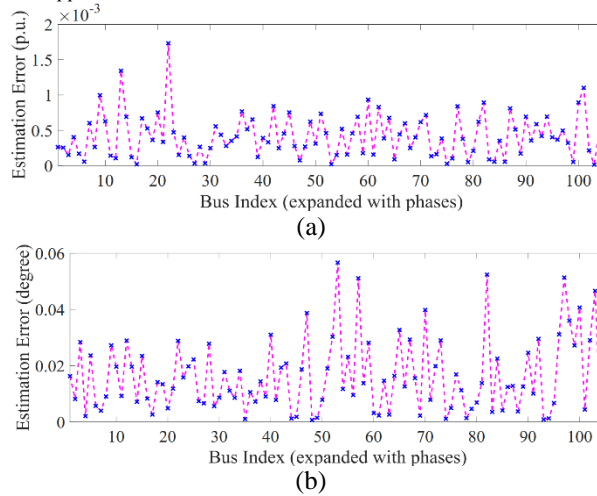


Fig. 5. Estimation errors for the IEEE 37-node system: (a) amplitude; (b) angle.

Tables:

TABLE 1. COMPARISON OF SE AMPLITUDE ERRORS.

TABLE 2. COMPARISON OF SE ANGLE ERRORS.

Table 3. COMPARISON OF COMPUTATION TIMES.

TABLE 4. NORMALIZED RESIDUALS OF NODE VOLTAGES IN SE ANALYSIS.

TABLE 5. NORMALIZED RESIDUALS OF ACTIVE POWERS IN SE ANALYSIS.

TABLE 6. NORMALIZED RESIDUALS OF REACTIVE POWERS IN SE ANALYSIS.

TABLE 7. MEASUREMENTS NUMBER.

TABLE 8. NORMALIZED RESIDUALS OF BUS VOLTAGES IN SE ANALYSIS.

TABLE 9. NORMALIZED RESIDUALS OF ACTIVE POWERS IN SE ANALYSIS.

TABLE 10. NORMALIZED RESIDUALS OF REACTIVE POWERS IN SE ANALYSIS

TABLE 1
COMPARISON OF SE AMPLITUDE ERRORS

Method	Index	37-node	123-node
Proposed Method	Mean Error	0.0053	0.0072
	Max Error	0.0066	0.0092
Three-Phase SDP	Mean Error	0.0061	0.0081
	Max Error	0.0073	0.011
Linear Method	Mean Error	0.0068	0.0091
	Max Error	0.0062	0.012

TABLE 2
COMPARISON OF SE ANGLE ERRORS

Method	Index	37-node	123-node
Proposed Method	Mean Error	0.1971	0.2615
	Max Error	0.5976	0.7863
Three-Phase SDP	Mean Error	0.3209	0.4231
	Max Error	0.6597	0.9745
Linear Method	Mean Error	0.5441	0.6789
	Max Error	0.8596	1.3718

Table 3
COMPARISON OF COMPUTATION TIMES

Method	37-node	123-node
Proposed Method	63 sec	263 sec
Three-Phase SDP	1623 sec	6185 sec
Linear Method	20 sec	64 sec

TABLE 4
MEASUREMENTS NUMBER

Node #	Phases	Node #	Phases	Node #	Phases
2	1-3	11	16-18	23	31-33
3	4-6	13	19-21	25	34-36
5	7-9	16	22-24	27	37-39
6	10-12	19	25-27		
8	13-15	21	28-30		

TABLE 5
NORMALIZED RESIDUALS OF NODE VOLTAGES IN SE ANALYSIS

Condition	Max Residual	Residual Sum
Without Bad Data	1.43	32.75
With Bad Data	18.1	79.8
After Bad Data Attenuation	2.3	47.58

TABLE 6
NORMALIZED RESIDUALS OF ACTIVE POWERS IN SE ANALYSIS

Condition	Max Residual	Residual Sum
Without Bad Data	1.22	40.5
With Bad Data	10.91	101.5
After Bad Data Attenuation	1.28	45

TABLE 7
NORMALIZED RESIDUALS OF REACTIVE POWERS IN SE ANALYSIS

condition	Max Residual	Residual Sum
Without Bad Data	1.2	38.6
With Bad Data	10.9	99.7
After Bad Data Attenuation	1.4	41.3

TABLE 8
NORMALIZED RESIDUALS OF BUS VOLTAGES IN SE ANALYSIS

Condition	Max Residual	Residual Sum
Without Bad Data	1.43	32.75
With Bad Data	34.6	158.3
After Bad Data Attenuation	2.45	49.95

TABLE 9
 NORMALIZED RESIDUALS OF ACTIVE POWERS IN SE ANALYSIS

Condition	Max Residual	Residual Sum
Without Bad Data	1.22	40.5
With Bad Data	21.1	189
After Bad Data Attenuation	1.35	48

TABLE 10
 NORMALIZED RESIDUALS OF REACTIVE POWERS IN SE ANALYSIS

condition	Max Residual	Residual Sum
Without Bad Data	1.2	38.6
With Bad Data	19.87	192
After Bad Data Attenuation	1.5	41.8